Sulphur dissociation in nuclear emulsion at 3.7 and 200A GeV

2002 J. Phys. G: Nucl. Part. Phys. 28 241

(http://iopscience.iop.org/0954-3899/28/2/305)

INSTITUTE OF PHYSICS PUBLISHING JOURNAL OF PHYSICS G: NUCLEAR AND PARTICLE PHYSICS

J. Phys. G: Nucl. Part. Phys. **28** (2002) 241–250 PII: S0954-3899(02)24048-7

Sulphur dissociation in nuclear emulsion at 3.7 and 200A GeV

M El-Nadi[1], A Abdelsalam[1], A Hussien[2], E A Shaat[1], N Ali-Mossa[3], Z Abou Moussa[1], S Kamel[4], K H Abdel-Waged[5] and M E Hafiz[4]

[1] Physics Department, Faculty of Science, Cairo University, Giza, Egypt
[2] Physics Department, Faculty of Science, Cairo University, Fayoum Branch, Fayoum, Egypt
[3] Basic Science Department, Faculty of Engineering, Banha Branch, Zagazig University, Banha, Egypt
[4] Physics Department, Faculty of Education, Ain Shams University, Cairo, Egypt
[5] Physics Department, Faculty of Science, Zagazig University, Banha, Egypt

Received 18 April 2001, in final form 19 September 2001
Published 21 January 2002
Online at stacks.iop.org/JPhysG/28/241

Abstract

In this work, the electromagnetic dissociation (EMD) of sulphur projectile induced by two widely differing energies in nuclear emulsions is investigated. Although the percentages of EMD events of the total numbers of studied interactions are relatively small, i.e. 5.7 and 14.4% for 3.7 and 200A GeV interactions respectively, one could extract some results out of them. The emission of a proton through the $^{32}S(\gamma, p)^{31}P$ channel is found to be a dominant process (43.8%) at 200A GeV whereas the single alpha emission through the $^{32}S(\gamma, \alpha)^{28}Si$ channel is the dominant one (34.0%) at 3.7A GeV. Multiplicity distributions of hydrogen and helium isotopes as well as the measured probabilities for the different modes of fragmentation are studied. The comparison of the present results, from electromagnetic and peripheral nuclear interactions, indicates the effective role of the different reaction mechanisms at ultra-relativistic energy (200A GeV). The experimental inclusive cross sections of different fragmentation modes produced in the EMD of ^{32}S ions at 200A GeV were found to be in satisfactory agreement with the predictions of the combined approach of Pshenichnov *et al*.

1. Introduction

The successful acceleration of heavy nuclei to ultra-relativistic energies opens up the possibilities of studying a variety of collision processes, depending upon the value of the impact parameter of the collision. Central collisions occurring at small impact parameters are most appropriate for investigating the highly excited and compressed hadronic matter and quark–gluon plasma. Peripheral collisions, taking place at large impact parameters, are used to study the fragmentation of projectile spectators. Whenever the impact parameters are beyond

the range of nuclear force, extremely strong electromagnetic fields are produced at the nucleus. In such interactions, the projectile is subjected to excitation by a short electromagnetic pulse provided by the electric charge of the target and enhanced by the Lorantz contraction [1].

The experiments carried out to study the electromagnetic dissociation [1–7] (EMD) in the virtual photon field of the target nucleus by relativistic heavy ions have an advantage over those using photons on a fixed target. This advantage arises from the fact that in the former case, the reaction fragments are emitted with the same rapidity as that of the beam so that they can be easily identified and measured.

The virtual photon flux and consequently the rate of photonuclear reaction are proportional to z^2, where z is the charge of the target nucleus. The EMD process is widely used for studying the properties of giant resonances (GRs) in nuclei, including multiphonon excitations [1].

The relative yields of the different modes of fragmentations and relationships between them are indicators of the processes that occur during the breakup of the projectile nucleus in the electromagnetic interactions. Consequently, this work focuses on:

(i) Studying some of these relationships which are observed in the EMD of ^{32}S projectiles at 3.7 and 200A GeV as well as investigating the dependence of the EMD mechanism on the incident energy.
(ii) Comparing the EMD relationships with those obtained in the peripheral nuclear interactions of the used ^{32}S beams [8, 9] in order to investigate the behaviour of nuclear matter under the effect of these two different mechanisms.
(iii) Comparing the experimental inclusive cross sections of different fragmentation modes produced in the EMD of 200A GeV ^{32}S with the corresponding values predicted according to the recently combined approach of Pshenichnov *et al* [10] which is designed specially for relativistic heavy ions with Lorentz factor $\gamma \gg 10$.

2. Experimental details

The present work is performed using two emulsion stacks of concentrations illustrated in table 1. The first stack was horizontally exposed to the 3.7A GeV ^{32}S ions at the Dubna synchrophasotron and the second one was tangentially irradiated by the 200A GeV ^{32}S ions of CERN-SPS. To obtain high scanning efficiency, the interactions of the incident beams were detected using the along-the-track scanning technique. The details about the irradiation and scanning are found in [11].

Table 1. The chemical composition of Br-2 and Fuji nuclear emulsions used for 3.7 and 200A GeV, respectively.

	Number of atoms $\times 10^{22}$ (cm^{-3})	
Element	Br-2	Fuji
H	3.150	3.2093
C	1.412	1.3799
N	0.395	0.3154
O	0.956	0.9462
S	–	0.0134
I	–	0.00552
Br	1.031	1.0034
Ag	1.036	1.0093

Once an interaction is observed, the incoming track is carefully examined to ensure that it is indeed a beam track and not one of the tightly bunched fragments of an undetected EMD event. In each interaction the multiplicity of grey tracks (N_g), black tracks (N_b), heavily ionized tracks ($N_h = N_g + N_b$), the tracks of the produced shower particles (N_S), the singly charged projectile fragments (N_H) and projectile fragments (PFs) of charge $Z \geqslant 2$ (N_Z) are recorded. These PFs are those produced within the fragmentation cone [3] defined by a critical angle θ_C, $\theta_C = 1$ mrad at 200A GeV and $\theta_C = 44$ mrad at 3.7A GeV. These values correspond to a spectator proton with a transverse momentum of 200 MeV/c. The angles of the PFs are measured using the coordinate method.

The pure EMD events are then selected to be analysed. Following [4], these events are characterized by having $N_h = 0$ and $N_S = 0$ (i.e. with no target nuclear excitation and no produced shower particles). On the other hand for each selected EMD event, the total charge of the produced PFs ($Z \geqslant 1$) must equal the charge of the incident beam. Exclusion of the low-energy electron pairs, high energy δ rays and the elastic scattering events was carried out [3, 11]. Since in nuclear emulsion only charged particles can be identified such that the charge of each but not the mass could be determined, neutrons cannot be detected and isotopes are not separated. Consequently, in this work the fragmentation modes ^{31}Sn, ^{30}S2n, ^{29}S3n, etc are not detectable and those having fragments accompanied with one or more neutrons are misidentified. Moreover ^{31}Sn disintegrations, expected to be as probable as ^{31}Pp ones, have escaped detection. Similarly, ^{30}Ppn cannot be distingushed from ^{31}Pp ones, and so on. The charge of each PF was determined by δ-ray counting, using the relation

$$N_\delta = A + BZ^2$$

where N_δ is the average number of δ rays per mm of the track length. The values of A and B were determined for each emulsion stack. The detection of $Z \leqslant 2$ PFs is quite definite due to their distinctive grain density in nuclear emulsion. Since this detector covers a 4π geometry and has a very high spatial resolution, it becomes an extremely useful identifying tool even when the fragmentation cone of the PFs is very narrow.

3. Results and discussion

In this research, it is found that among a total of 827 and 1459 interactions of ^{32}S beams with emulsion nuclei at 3.7 and 200A GeV, 47 (5.7%) and 210 (14.4%) pure EMD events are detected, respectively. Such percentage increase shows a clear dependence of the production of EMD events on the projectile's energy. The present result for the 200A GeV ^{32}S beam agrees quite well with that obained by the Buffalo group [3].

The normalized charge spectra of all PFs having charge from $Z = 1$ to $Z = 15$ for the 3.7 and 200A GeV ^{32}S beams are presented in figure 1. For the two used energies, it is noticed that the most abundant PF is that with charge $Z = 1$ and the next one is that with $Z = 2$. The least abundant charges are those in the ranges $3 \leqslant Z \leqslant 13$, after which there is an increase in the relative abundance. For 200A GeV, the ratio of PFs with charge $Z = 1$ to those with charge $Z = 2$ is almost 2.5 while the corresponding ratio in the case of 3.7A GeV is only 1.5. The PFs of charge $Z = 15$ have relative yields of almost 1.8 and 0.7 times those with $Z = 14$ for 200 and 3.7A GeV, respectively. These charge spectra enable one to determine the decay modes of the observed channels.

In tables 2 and 3 the different visible decay modes (i.e. those involving charged fragments ($Z = 1$, 2, etc)) of ^{32}S dissociation at 200 and 3.7A GeV are tabulated. From this table, it is noticed that only 28 and 10 channels have been observed for 200 and 3.7A GeV ^{32}S beams, respectively. Although the authors of [4] stated that sulphur, with a binding energy of

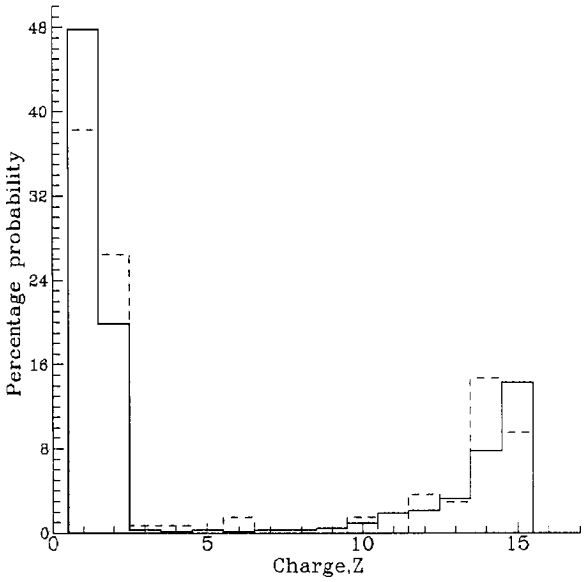

Figure 1. Normalized charge spectra of the PFs with $1 \leqslant Z \leqslant 15$ emitted in EMD events for ^{32}S at 200A GeV (solid line) and 3.7A GeV (dashed line).

8.5 MeV per nucleon, can disintegrate into more than 200 channels, they also detected at 200A GeV only 28 channels. In addition to the different decay modes, tables 2 and 3 also show: (i) the threshold energy [6] in MeV, $E_{\rm th}$, for the excitation of a given mode calculated in the rest frame of the projectile by using the mass defect formula [12], and (ii) the number of EMD events, $N_{\rm EMD}$, observed for each mode of decay and its percentage relative rate. For the sake of comparison, the corresponding relative rates from [3, 4] for ^{32}S beams at 200A GeV are given in table 2. It can be seen that the present results show a fair agreement, within the statistical errors, with the compared ones.

From tables 2 and 3, one can also observe that among the visible channels, the emission of a proton through the ^{32}S(γ, p)^{31}P channel is the dominant process (43.8%) at 200A GeV, whereas at 3.7A GeV the single alpha emission (through the ^{32}S(γ, α)^{28}Si channel) is the dominant one (34.0%).

Figure 2 represents the proportion of decay modes, Y, of ^{32}S projectiles at the two used energies as a function of the threshold energy, $E_{\rm th}$, for all EMD events given in tables 2 and 3. This figure indicates that the dependence on threshold energy at the two used ^{32}S energies seems to be approximately the same for the various break-up channels. This means that almost all the possible modes of decay occur independently of the energy of the incident projectile as was previously found by Bahk *et al* [13]. The experimental data which are presented in figure 2 can be fitted by the relation $Y = \exp(AE_{\rm th} + B)$ where, $A = -0.035 \pm 0.004\,{\rm MeV}^{-1}(\chi^2/{\rm DOF} = 2.1)$, and $A = -0.039 \pm 0.003\,{\rm MeV}^{-1}(\chi^2/{\rm DOF} = 2.4)$ at 200 and 3.7A GeV, respectively (DOF denotes degrees of freedom). It is noticed that the values of A determined in this work are nearly equal, within errors, to those of [6, 13].

Table 4 displays the emission relative rates of single proton (mode (1)) and single alpha (mode (2)) channels for the present ^{32}S dissociation at 3.7 and 200A GeV compared to the corresponding results of ^{16}O dissociation at 3.7A GeV of [14] and at 200A GeV of [4]. The findings of this table can clarify that, at the same energy, the rate of single-proton emission decreases as the mass number of projectile increases. On the other hand, the single-alpha

Table 2. Different decay modes for ^{32}S, threshold energy (E_{th}), observed number of EMD events (N_{EMD}) and EMD relative rates at 200A GeV.

Decay mode	E_{th} (MeV)	N_{EMD}	Relative rate (%) This work	[3]	[4]
^{31}P + p	8.86	92	43.8 ± 4.6	37.7 ± 4.4	53.8 ± 3.4
^{28}Si + α	6.94	30	23.8 ± 3.4	26.7 ± 3.7	29.2 ± 2.5
^{28}Si + 2d	30.78	20			
^{27}Al + α + p	18.54	15	10.0 ± 2.2	10.5 ± 2.3	6.8 ± 1.2
^{27}Al + 2d + p	42.37	6			
^{24}Mg + 2α	16.96	5	6.7 ± 1.8	8.9 ± 2.2	3.8 ± 0.9
^{24}Mg + α + 2d	40.79	4			
^{24}Mg + 4d	64.63	5			
^{23}Na + 2α + p	28.71	4	5.7 ± 1.7	2.1 ± 1.0	1.3 ± 0.7
^{23}Na + ^{7}Li + 2p	46.05	1			
^{23}Na + α + 2d + p	52.55	4			
^{23}Na + 4d + p	76.38	3			
^{20}Ne + 2α + 2d	50.09	3	2.9 ± 1.2	2.6 ± 1.2	0.9 ± 0.5
^{20}Ne + α + 4d	73.93	3			
^{19}F + 2α + 2d + p	62.96	1	1.4 ± 0.8	3.1 ± 1.3	1.3 ± 0.7
^{19}F + 3α + p	39.13	2			
^{16}O + 3α + 2d	54.85	1	1.9 ± 0.7	5.2 ± 1.7	1.9 ± 0.9
^{16}O + 2α + 4d	78.68	1			
^{14}N + 3α + 3d	75.57	1			
^{14}N + 2α + 5d	99.40	1			
^{12}C + 3α + 4d	85.83	1	2.3 ± 1.2	2.1 ± 1.0	1.0 ± 0.7
^{11}B + 4α + 2d + p	77.95	1			
^{11}B + 2α + 6d + p	125.62	1			
^{9}Be + 2α + 7d + p	141.43	1			
^{7}Li + 4α + 4d + p	110.44	1			
6α + 4d	93.11	1	1.4 ± 0.8	1.0 ± 0.8	0.6 ± 0.5
5α + 6d	116.94	1			
4α + 8d	140.78	1			

Table 3. Different decay modes for ^{32}S, threshold energy (E_{th}), observed number of EMD events (N_{EMD}) and EMD relative rates at 3.7A GeV.

Decay made	E_{th} (MeV)	N_{EMD}	Relative rate (%)
^{31}P + p	8.86	13	27.66 ± 7.67
^{28}Si + α	6.94	16	42.55 ± 9.52
^{28}Si + 2d	30.78	4	
^{27}Al + α + p	18.54	4	8.51 ± 4.25
^{24}Mg + α + 2d	40.79	3	10.64 ± 4.76
^{24}Mg + 4d	64.63	2	
^{20}Ne + 2α + 2d	50.09	2	10.64 ± 4.76
2 ^{12}C + 2α	30.88	1	
^{9}Be + 3α + 5d + p	117.6	1	
^{7}Li + 5α + 2d + p	86.61	1	

emission has an inverse yield, i.e. it increases with the increase of projectile mass number. It can be noted that these relative rate changes occur more rapidly at the lower used energy (3.7A GeV) which is clearly demonstrated in the ratio of mode (1) to mode (2). This table

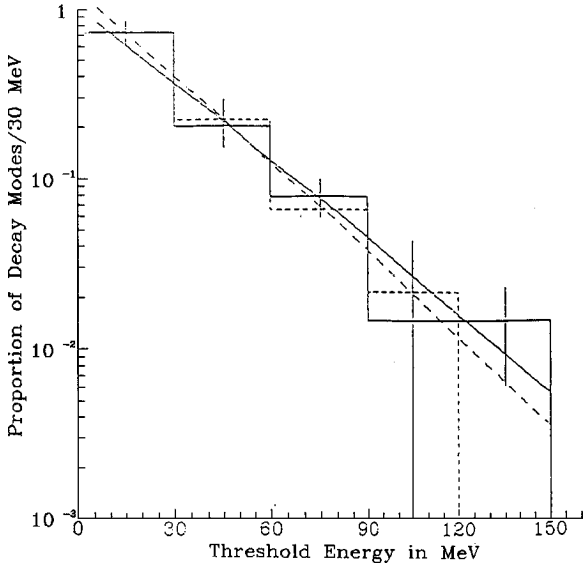

Figure 2. Proportion of decay modes as a function of the threshold energy (in MeV) for ^{32}S dissociation at 200A GeV (solid histogram) and 3.7A GeV (dashed histogram). The corresponding lines are the least square fit of the data points, respectively.

Table 4. Relative rates of visible channels of single proton and single alpha together with the ratio between them for EMD of ^{16}O and ^{32}S at 3.7 and 200A GeV.

	3.7A GeV ^{16}O	3.7A GeV ^{32}S	200A GeV ^{16}O	200A GeV ^{32}S
Decay mode	[14]	This work	[4]	This work
(1) Single proton	42.2 ± 6.2	27.7 ± 7.7	56.0 ± 4.0	43.8 ± 4.6
(2) Single alpha	5.5 ± 2.2	34.0 ± 8.5	10.0 ± 2.0	14.3 ± 2.6
Ratio of mode (1) to mode (2)	7.7 ± 1.1	0.8 ± 0.2	5.6 ± 0.7	3.1 ± 0.5

also shows that the effect of increasing the energy from 3.7 to 200A GeV on the ratio of the yield of single proton to that of single alpha is only clear (within the experimental errors) for the heavier projectile (i.e. ^{32}S).

A detailed study of energy spectra for the channels observed in the EMD of sulphur nuclei at 200A GeV would be a much more reliable test to understand the electromagnetic excitation mechanism at ultrarelativistic energy. This study is now under preparation for publication [15].

In the present experiment and owing to the collection of exclusive data, it was possible to study $Z = 1$ and $Z = 2$ fragment distributions and correlations. Very recently in [16], the reaction channel ^{32}S (γ, p) ^{31}P at 200A GeV has been studied where it is found that the majority of events in this channel may be attributed to the absorption of giant dipole resonances. In case of hydrogen isotopes, the present average multiplicities of $(Z = 1)$ fragments, $\langle N_{\mathrm{H}} \rangle$, emitted in the two EMD samples at 3.7 and 200A GeV are found to be nearly the same, (1.76 ± 0.15) and (1.73 ± 0.32), respectively. Their multiplicity distributions are plotted in figure 3, showing that as the number of the emitted $(Z = 1)$ fragments, N_{H}, per event increases, the percentage probability of its production decreases. This figure also shows that in the case of 200A GeV, the production probabilities extend to higher multiplicity values of N_{H} (up to 8). This may reflect the dependence of the dissociation degree of an interaction on the projectile energy. In figure 4, the multiplicity distributions of He PFs emitted in the present EMD events at the

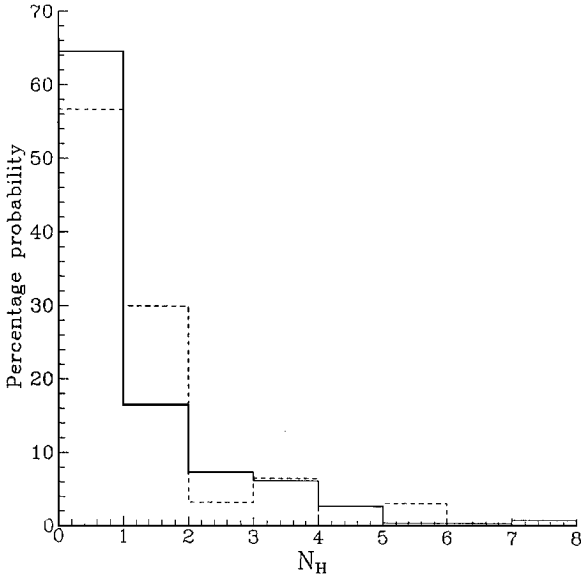

Figure 3. Multiplicity distributions of hydrogen isotope ($Z = 1$) fragments emitted in the EMD events of ^{32}S–Em interactions at 200A GeV (solid line) and 3.7A GeV (dashed line).

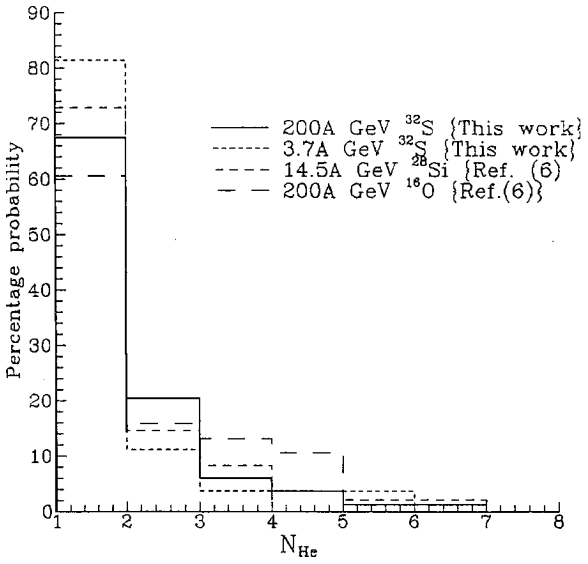

Figure 4. Multiplicity distributions of He-fragments emitted in the EMD of different projectiles with different energies in emulsion.

two used energies together with the corresponding distributions of [6] for 14.5A GeV ^{28}Si and 200A GeV ^{16}O data seem to be very similar. It is obvious that the behaviour of the decreasing yield of alpha emitted in EMD process neither depends on the projectile mass number nor on its energy. Moreover, this behaviour does not depend on the He-production mechanism (whether EMD or nuclear interactions) for 3.7 and 200A GeV ^{32}S–Em collisions as shown recently in [17].

Table 5. Some parameters describing the sulphur fragmentation from EMD and nuclear peripheral interactions in emulsion at 3.7 and 200A GeV, respectively.

	Probability (%) for different fragmentation modes			
	3.7A GeV		200A GeV	
Fragmentation mode	EMD	Nuclear	EMD	Nuclear
Two fragments with $Z > 2$	2.13 ± 2.13	2.50 ± 1.40	0.48 ± 0.48	2.24 ± 0.53
One fragment with $Z > 2$	97.87 ± 4.43	87.50 ± 8.50	98.10 ± 6.83	62.76 ± 2.80
Fragments with $Z > 2$ and no α particles	40.43 ± 9.27	30.80 ± 5.10	60.48 ± 5.37	31.34 ± 2.80
Fragments with $Z > 2$ and α particle	59.57 ± 11.25	59.20 ± 7.00	38.09 ± 4.16	33.66 ± 2.90
α particle and no heavier fragments	0.00	10.00 ± 2.89	1.42 ± 0.82	34.69 ± 2.94

In order to understand the dynamics of projectile fragmentation for interactions occurring at large impact parameters, an investigation is carried out using the present data concerning the 3.7 and 200A GeV EMD events together with the corresponding results for the peripheral nuclear collisions. The latter results are calculated from the data presented in [8, 9] at 3.7 and 200A GeV, respectively. Table 5 illustrates the probabilities (in percentage) for the different fragmentation modes of the present ^{32}S EMD events at the two used energies compared to the corresponding results for the peripheral nuclear samples. From this table, the measured percentage probabilities indicate that:

(a) The production of a single fragment with $Z > 2$ in the case of EMD events, which is the most probable mode of fragmentation, has nearly the same probability at the two used energies. On the other hand in the case of nuclear samples, the production of this mode decreases with energy.
(b) The probability of producing fragments of $Z > 2$ without the production of α particles increases with the increase of energy in the case of EMD process while such probability for the nuclear interactions is independent of energy.
(c) At the two used energies, the production of $Z > 2$ fragments accompanied by α particles seems to be independent of the mechanism of interaction whether EMD or nuclear. However such production decreases with increasing energy.
(d) In the case of nuclear process, the probability of producing α particles without being accompanied by heavier fragments increases with energy. On the other hand, for the EMD process at the two used energies, such probability nearly vanishes.

Figure 5 represents the experimental inclusive cross sections of the different fragmentation modes produced in the EMD of ^{32}S ions at 200A GeV ($\sigma(Z)$) as a function of the fragment's charge (z) along with the combined model calculations [18]. The experimental points presented in this figure are deduced from table 2 with the use of the following relation [6]:

$$\sigma_{\mathrm{EMD}} = f_{\mathrm{Ag}} / N_{\mathrm{Ag}} \lambda$$

where σ_{EMD} is the total production cross section for EMD events due to the Ag target, f_{Ag} is the weight factor of Ag nuclei (=0.62), N_{Ag} is the concentration of Ag nuclei in the used emulsion (table 1) and λ is the EMD mean free path [15] (=40.1 $\pm$ 2.7 cm), corrected for the undetectable disintigration modes.

According to the above relation the experimental σ_{EMD} equals (1531 $\pm$ 103) mb.

The combined model with which the present data are compared assumes three steps. In the first step, the energy of a virtual photon is simulated according to the Weizsacker–Williams (WW) method [19]. The second step is the nuclear photoabsorption process which

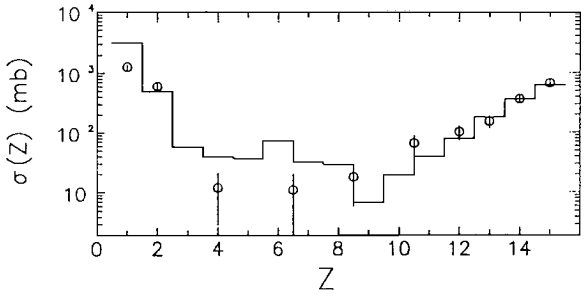

Figure 5. Inclusive cross sections of the different fragmentation modes in the EMD of 200A GeV ^{32}S ions as a function of the fragment's charge (z). Circles are the present experimental data. The histogram is the prediction of the combined model [18].

is treated on the basis of the intranuclear cascade (INC) model [20]. In the used version of INC, the elementary γN interaction (N refers to a nucleon) has been developed taking into account both the resonance contributions from the two-body channels $\gamma\mathrm{N} \to \pi\mathrm{B}^*$ and $\gamma\mathrm{N} \to \mathrm{M}^*\mathrm{N}$ (B^* and M^* are baryon and meson resonances, respectively) and the non-resonant statistical contribution from multibody channels $\gamma\mathrm{N} \to i\pi\mathrm{N}$ ($2 \leqslant i \leqslant 8$). At sufficiently high photon energies many hadrons are produced inside a nucleus in the course of a cascade process. Finally, the excited residual nuclei formed after the completion of the intranuclear cascades undergo de-excitation. This latter process is described by the statistical multifragmentation model (SMM) [21].

The combined approach yields [18] a value of 1643 mb for σ_{EMD} of the 200A GeV ^{32}S on Ag nuclei. Although the overall experimental and theoretical values σ_{EMD} are in a reasonable agreement, figure 5 shows that for $3 < z < 7$ the combined model overestimates the experimental inclusive cross sections of the different fragmentation modes. However, the experimental data presented in figure 5 are generally in satisfactory agreement with the predictions of the combined model.

4. Conclusions

In the present work, the electromagnetic dissociation of ^{32}S projectile in nuclear emulsions at 3.7 and 200A GeV is investigated. Although the percentage of visible EMD events of the total number of studied interactions is relatively small, 5.7 and 14.4% for the two used energies, respectively, one could extract the following conclusions:

(1) The present data show a clear dependence of the production of the EMD events on the projectile's energy.
(2) The emission of a proton through the ^{32}S (α, p)^{31}P channel was found to be the dominant process (43.8%) at 200A GeV whereas the single alpha emission was found to be dominant (34.0%) at 3.7A GeV.
(3) At constant incident energy per nucleon (whether 3.7 or 200A GeV), the production of single proton decreases as the projectile's mass number increases. However, such increase is more obvious at the lower energy. On the other hand, single alpha emission has an inverse yield.
(4) The present average multiplicities of $Z = 1$ PFs, $\langle N_{\mathrm{H}} \rangle$, emitted in the two EMD samples at the two used energies exhibit an energy independence. Similar result was obtained in [17] for $Z = 2$ PFs in EMD interactions. However, by investigating $Z = 1$ PF multiplicity

distributions, it is found that, in case of 200A GeV, the distribution extended to higher values of N_H (up to 8), which may reflect the effect of the projectile's energy on the dissociation degree of an interaction.

(5) In the case of He-multiplicity distributions, the behaviour of the helium production yield neither depends on the mass number nor on the energy of the projectile.

(6) In the case of EMD events it can be observed that:

(a) The production of a single fragment having $Z > 2$ with or without being accompanied by α particles and which is the most probable mode of fragmentation, has nearly the same probability at the two used energies.

(b) For the events where $Z > 2$ fragments are the only emitted ones, the production probability increases with increasing energy. This observation is reversed for the events where α particles are also emitted.

(7) The present inclusive cross sections of the different fragmentation modes at 200A GeV could be described by the approach of Pachenichnov *et al* [18] in which the INC and SMM models are combined.

Finally, the electromagnetic fields generated by ultra-relativistic heavy ions are so strong that one can expect qualitatively new phenomena in such collisions. Nuclear multifragmentation is only one example of rich possibilities.

Acknowledgments

The authors express their gratitude to the authorities of CERN SPS for irradiation of the plates. We are also grateful to the staff of the synchrophasotron at JINR Dubna, for their help in the exposure of the emulsion stacks.

References

[1] Bertulani C A and Baur G 1988 *Phys. Rep.* **163** 299; and references therein
[2] Brechtmann C and Heinrich W 1988 *Z. Phys.* A **330** 407
[3] Singh G, Sengupta K and Jain P L 1990 *Phys. Rev.* C **41** 999
[4] Baroni G *et al* 1990 *Nucl. Phys.* A **516** 673
[5] Barette J *et al*, E 814 Collaboration 1990 *Phys. Rev.* C **41** 1512
[6] Singh G and Jain P L 1992 *Z. Phys.* A **344** 73
[7] Nabil Yasin M 1995 *IL Nuovo Cimento* A **108** 1041
[8] Fayed M 1996 *MSc Thesis* Cairo University
[9] Shaat E A 1994 *Egypt J. Phys.* **25** 147
[10] Pshenichnov I A *et al* 1999 *Phys. Rev.* C **60** 044901
[11] El-Nadi M *et al* 1997 *Int. J. Mod. Phys.* E **6** 191
El-Nadi M *et al* 1996 *IL Nuovo Cimento* A **109** 1517
[12] Kaplan I 1962 *Nuclear Physics* 2nd edn (Reading, Mass: Addison-Wesley) Chapter 9 p 221
[13] Bahk S Y *et al* 1991 *Phys. Rev.* C **43** 1410
[14] Nabil Yasin M *et al* 1997 *JETP* **84** 635
[15] El-Nadi M *et al* unpublished
[16] Kamel S 1999 *IL Nuovo Cimento* A **112** 327
[17] Kamel S 1999 *IL Nuovo Cimento* A **112** 733
[18] Pshenichnov I A *et al* 1998 *Phys. Rev.* C **57** 1920
[19] Jackson J D 1975 *Classical Electrodynamics* 2nd edn (New York: Wiley)
[20] Iljinov A S *et al* 1997 *Nucl. Phys.* A **616** 575
[21] Bondorf J P *et al* 1995 *Phys. Rep.* **257** 133